Analyst

RSC Publishing

PAPER

View Article Online
View Journal | View Issue

Cite this: *Analyst*, 2013, **138**, 2964

Role of three-body recombination for charge reduction in MALDI process

Yiming Lin, Zhibin Yin, Xiaohua Wang, Weifeng Li and Wei Hang*

Ions in Matrix-Assisted Laser Desorption/Ionization (MALDI) are predominantly singly charged for small analyte molecules. With the estimated high number density and low temperature of electrons, the three-body recombination mechanism is attractive and should be considered as an important cause for the charge reduction in the plume. Theoretical calculations indicate that the rate coefficient of the three-body recombination is about 50 times higher than that of the two-body recombination if the analyte molecule has insufficient degrees of freedom. Experimental results show that, for small analyte molecules, the ratio of AH_2^{2+}/AH^+ is close to the theoretical 5% value from the three-body recombination modeling and this ratio declines with the increasing electron and matrix molecule number density caused by greater laser irradiance. The ratio of $[A + 2]^+/[A + 1]^+$ is higher than the theoretical isotopic value, and the excess $[A + 2]^+$ could exclusively result from the three-body recombination collisions. Further evidence demonstrates that $[A + 2]^+/[A + 1]^+$ increases with electron number density, which is in correspondence with the model. All of these theoretical and experimental results indicate that three-body recombination is an essential charge reduction mechanism for small molecules in the MALDI plume.

Received 26th November 2012
Accepted 2nd March 2013

DOI: 10.1039/c3an36749e

www.rsc.org/analyst

Introduction

Matrix-assisted laser desorption/ionization (MALDI) has been widely used for mass spectrometric analysis of non-volatile large molecules, particularly biomolecules and synthetic polymers.[1] In spite of the considerable development and application of MALDI, the fundamental nature of the mechanisms involved in MALDI processes remain poorly understood. Neither a simple chemical nor physical model can be applied for illustrating the complex processes from the condensed phase to the diluted gas phase and finally the ion formation. In addition, a great variety of experimental conditions, including laser parameters, sample preparation methods, and the types of analyte and matrix molecules, should be considered in the MALDI ionization mechanism.

Two major processes are commonly accepted in MALDI ionization: primary and secondary ion formation. During or shortly after the laser pulse, primary ions are generated from neutral molecules, which are often matrix species. In the ensuing desorption/ablation plume expansion, ion–molecule reactions give rise to the most favorable secondary ions through conversion of the primary ions. In particular, analyte ions are formed *via* the secondary reaction, which dominates the final detected mass spectrum. The role of an individual mechanism in the two processes remains debatable. Energy pooling[2,3] cluster models,[4,5] multiphoton ionization,[6,7] excited-state proton transfer,[8] and thermal ionization models[9] were applied as mechanisms for primary ion formation. For the in-plume processes of the secondary reaction, proton transfer, electron transfer, cation transfer, and electron capture are potential candidate events.[10] Advances in molecular dynamics simulations have provided rational and predictive foundations for the experimental results.[2,3,11]

Whatever the experimental or modeling approaches, a better understanding of ion formation in MALDI is extraordinarily important to improve the control of ion yield, charge state, fragmentation, and for using MALDI to analyze new classes of compounds. An interesting phenomenon in MALDI events is that singly charged ions are the major ion type for small molecules. The cluster model was proposed for the ion formation, and electron capture neutralization accompanied by electron capture dissociation of highly charged ions was pointed out for the charge reduction and molecule fragmentation.[5] Electrons are thought to be important in suppressing the yield of multiply charged ions. However, in-plume secondary ion–molecule reactions are believed to be much more likely than the electron capture process because the plume is under thermodynamic rather than kinetic control.[12] While not ruling out the events mentioned above, we suggest that the mechanism of three-body recombination contributes to the detection of mostly singly charged ions in MALDI mass spectra. The three-body recombination mechanism is favorable based on two factors: the electron density and recombination rate coefficient, which will be discussed below.

Department of Chemistry and The Key Laboratory of Analytical Sciences, College of Chemistry and Chemical Engineering, Xiamen University, Xiamen 361005, China. E-mail: weihang@xmu.edu.cn

Experimental

In the experiment, a commercial MALDI time-of-flight mass spectrometer (microFlex, Bruker Daltonics) equipped with a nitrogen laser (337 nm) was operated in reflection and positive ion mode. Acceleration voltage was set at 20 kV. Since low irradiance results in little signal and high irradiance deteriorates the spectral resolution, the laser irradiance can only be in a range of 4×10^7 to 2×10^8 W cm^{-2}. However, this range is enough to illustrate the trends of signals with the change in irradiance. The experimental conditions were carefully controlled in this research. Since the laser energy is the most important factor, only the laser irradiance was changed while the other conditions were all kept the same.

The two most common matrices, DHB (2,5-dihydroxybenzoic acid) and CHCA (α-cyano-4-hydroxycinnamic acid), were used. MALDI targets were prepared by the standard "dried droplet" method by mixing 1 μl of analyst solution (0.015 mg ml^{-1}) and 1 μl of matrix saturated in water–acetonitrile–formic acid (50 : 50 : 0.1 v/v/v). The matrices DHB and CHCA were purchased from Bruker Daltonics (Bremen, Germany), and all of the high-purity solvents were obtained from Fluka (Buchs, Switzerland). Peptide A with the sequence Phe-Leu-Lys-Ile-Lys-Arg-Asn-Asp-Glu-Thr-Val was self-synthesized and dissolved in water–formic acid (100 : 0.1 v/v). Bacitracin A and lysozyme were purchased from GL Biochem Ltd (Shanghai, China). A peptide calibration standard (Part no. #206195, Bruker Daltonics, Bremen, Germany) was applied for external calibration. For convenience, the matrix and analyte molecules are denoted as M and A, respectively.

Results and discussion

Theoretical consideration

In MALDI ionization processes, the role of the matrix is to absorb the laser energy, release it by inter- or intra-molecular relaxation and finally to cause the sample to disintegrate. During or shortly after the laser pulse, when the energy is highly concentrated, is the only time scale for charge separation. Thus, the electrons are generated in the primary ion formation procedure through multiphoton ionization:[6]

$$\mathrm{M} \xrightarrow{h\nu} \mathrm{M}^* \xrightarrow{h\nu} \mathrm{M}^{+\cdot} + \mathrm{e}^- \quad (1)$$

which is a straightforward pathway for electron emission.

Another mechanism called energy pooling is also an attractive model for electron generation.[2,13–15] In this model, energy redistribution occurs between two nearby electronic excited molecules through wavefunction overlap. The coupled system of two neighboring excited-state matrix molecules will pool their energies to yield one matrix radical cation and one neutral molecule in the ground state, emitting one electron:

$$\mathrm{MM} \xrightarrow{2h\nu} \mathrm{M}^*\mathrm{M}^* \longrightarrow \mathrm{M} + \mathrm{M}^{+\cdot} + \mathrm{e}^- \quad (2)$$

Proton transfer is a well-known mechanism for the formation of singly charged analyte molecules. For multiply charged analyte ions with the charges far apart, the internal electrostatic repulsion will be sufficiently low, and the ions will remain multiply charged stably.[14,16]

The most important route for highly charged ion formation is the proton transfer reaction:

$$\mathrm{MH}^+ + \mathrm{AH}^+ \rightarrow \mathrm{AH_2}^{2+} + \mathrm{M} \quad (3)$$

$$\mathrm{MH}^+ + \mathrm{AH_2}^{2+} \rightarrow \mathrm{AH_3}^{3+} + \mathrm{M} \quad (4)$$

Doubly charged analyte ions are generated through proton transfer from protonated matrix ions to singly protonated analyte ions, with triply charged ions following a similar mechanism.[17] The proton affinity (PA) of matrix and analyte ion species could determine the final yield of multiply charged ions.[17] If the PA value of the protonated analyte ion is higher than that of the matrix ion, exothermicity of reaction is expected and highly charged analyte ion will be generated. Conversely, the increase of the charge state will also decrease the PA value due to internal coulombic repulsion.[18] Although the formation of highly charged ions is thermodynamically favorable, the ions are always reduced to the +1 charge state. If the charge state is higher, the reduction is more efficient.

Electrons are thought to play a significant role in the reduction process and influence the yield of multiply charged ions. The laser fluence and matrix ionization potential are two straightforward aspects.[19] On the one hand, as the laser power increases, the electron density also increases because of the multiphoton ionization. On the other hand, matrix molecules with lower ionization potential will be more easily ionized and generate more electrons. Both factors tend to cause the charge reduction and decrease the yield of multiply charged ions.

After the ionization of matrix molecules, electrons are emitted from the surface layer of the sample, resulting in the buildup of surface charging, and the generation of an electric field of approximately 10^8 V m^{-1}. The electron energy is insufficient to overcome the field barrier. The electrons will be drawn close to the surface layer rather than escape into the vacuum.[20] The timescale required for plume expansion to collision-free density may be many microseconds. During this period, the average neutral number density in the plume is approximately 10% of the pre-desorption solid.[10] The total neutral number density in the solid phase is 6×10^{21} cm^{-3}; thus, this number should be 6×10^{20} cm^{-3} in the gas phase. Through the calculation,[20] the electron fractional emission is 1.5×10^{-2}. As a result, the electron density can reach as high as 9×10^{18} cm^{-3} in the plume. The electron temperature is also assumed to be important to the rate coefficient of the three-body recombination. Under typical MALDI conditions, the local thermal equilibrium is reached at a plume temperature of about 500 K.[2,14] During adiabatic expansion, frequent collisions occur, and the plume cools rapidly. Thus, the electron temperature is assumed to be lower than 0.1 eV, which could lead to a high rate coefficient for the three-body recombination.

The three-body recombination mechanism, also called collisional-radiative recombination, is an attractive model because of the great recombination rate at high electron density ($n_e > 10^{12}$ cm^{-3}) and low electron temperature.[21] This process involves one ion, one electron, and a third body, either an electron or a matrix molecule, as an energy carrier. Here, we use a doubly charged ion as an example for the three-body recombination process:

$$AH_2^{2+} + e^- + e^- \rightarrow AH^+ + H^{\cdot} + e^- \quad (5a)$$

$$AH_2^{2+} + e^- + M \rightarrow AH^+ + H^{\cdot} + M \quad (5b)$$

or

$$AH_2^{2+} + e^- + e^- \rightarrow AH_2^+ + e^- \quad (6a)$$

$$AH_2^{2+} + e^- + M \rightarrow AH_2^+ + M \quad (6b)$$

The hydrogen radical can be released (as eqn (5a) or (b)) or remain at the high proton affinity site of the analyte molecule (as eqn (6a) or (b)). The estimated rate coefficient k_{3b} is given by:[22]

$$k_{3b} = a\rho T_e^{-5} n_e \text{ cm}^3 \text{ s}^{-1} \ (T_e < 3100 \text{ K}) \quad (7)$$

where T_e is the electron temperature, n_e is the electron number density, a is a constant related to the ion type (a is $\sim 1 \times 10^{-6}$ for most ions because it is related to the ratio of collisional cross-section and molecular weight),[23,24] and ρ is the Coulomb logarithm given by:

$$\rho = z^3 \ln(z^2 + 1)^{1/2} \quad (8)$$

with z being the charge state. When $T_e = 0.1$ eV, the calculated k_{3b} is 5.8×10^{-2} cm^3 s^{-1} for AH_2^{2+}.

The k_{3b} value is compared to the rate coefficient of the two-body recombination process as:

$$AH_2^{2+} + e^- \rightarrow AH^+ + H^{\cdot} \quad (9)$$

The doubly charged analyte ion captures an electron and becomes a singly charged ion. The excess energy is preferably released with the emitted hydrogen radical and redistributed among the molecular internal degrees of freedom if the molecule is large enough. The rate coefficient is expressed as:[25]

$$k_{2b} = \sigma V = \pi r_c^2 V = \pi \left(\frac{8k'e^2}{3kT_e}\right)^2 \sqrt{2kT_e/m_e} \quad (10)$$

where σ is the electron capture cross-section, V is electron velocity, k is the Boltzmann constant, and m_e is the electron mass. The capture cross-section can be deduced from the capture radius (r_c), which is defined as the distance at which the ion–electron electrostatic potential energy is equal to the kinetic energy of the electrons:

$$r_c = \frac{8k'e^2}{3kT_e} \quad (11)$$

where k' is the electrostatic constant and e is the electron charge. Thus, for doubly charged ions at $T_e = 0.1$ eV, the two-body recombination rate coefficient is $k_{2b} = 1.1 \times 10^{-3}$ cm^3 s^{-1}. This value is 50 times lower than the k_{3b} value (5.8×10^{-2} cm^3 s^{-1}) for the three-body recombination. Theoretically, the three-body recombination mechanism will substantially overtake the two-body recombination.

Under the same electron temperature and number density, the three-body recombination rate coefficient for the same ion type with different charge states can be compared qualitatively by the Coulomb logarithm value ρ. From eqn (7), k_{3b} is linearly proportional to ρ, while ρ is equal to $z^3\ln(z+1)^{1/2}$, given by eqn (8). Thus, it can be calculated that k_{3b} of the +2 charge state is approximately 20 times higher than that of the +1 charge state. In other words, the probability that the +2 charge state will be reduced to +1 is approximately 20 times higher than that of the +1 charge state being neutralized to +0. This result means that the final number density of doubly charged ions is only 1/20 (~5%) of the singly charged ions to achieve an equal recombination rate. If the number density of the doubly charged ions is in excess, its higher recombination rate will cause them to be further reduced to the +1 charge state until the 5% value is reached finally.

Experimental proof

The peptide A and bacitracin A used in our experiment possess 4 (including N-terminal) and 2 protonation sites, respectively. From Fig. 1, the intensity ratios AH_2^{2+}/AH^+ of peptide A are about 4.6% in the DHB matrix and 4.1% in the CHCA matrix, while for bacitracin A, the AH_2^{2+}/AH^+ ratios are 6.4 and 5.2% in the two matrices, respectively. All these ratios are close to the 5% value predicted in the three-body recombination modeling. In other groups' work, peptides of mass ~2000 with 1 and 6 protonation sites have AH_2^{2+}/AH^+ values of 4.6 and 4.2%, respectively,[19,26] which strongly supports our prediction of the three-body recombination mechanism for charge reduction.

From eqn (5) and (6), it can be deduced that the amount of AH_2^{2+} will be decreased with the increase of electron and matrix molecule number densities. Peptide A was chosen as a model for further experiments, since it has a simple structure and incurs less complicated processes. From Fig. 2, it can be observed that the ratio of AH_2^{2+}/AH^+ decreases with the increase in laser irradiance, since more three-body collisions will occur with the increase in electron and matrix molecule number densities. The trends of AH_2^{2+}/AH^+ change as predicted, and the ratios start to level off at a laser irradiance greater than 1.4×10^8 W cm^{-2}. This experimental result provides the second evidence suggesting the three-body recombination as an important charge reduction mechanism for small analyte molecules.

The third evidence is that if the H$^{\cdot}$ is not released from the backbone of the molecule (eqn (6a) and (b)), AH_2^+ ions will be generated. The isotopic distribution will change with the intensity ratio of $[A + 2]^+/[A + 1]^+$ to become greater than the theoretical value (74%) for peptide A. With respect to $[A + 1]^+$, 4.2 and 4.5% more $[A + 2]^+$ in DHB and CHCA, respectively,

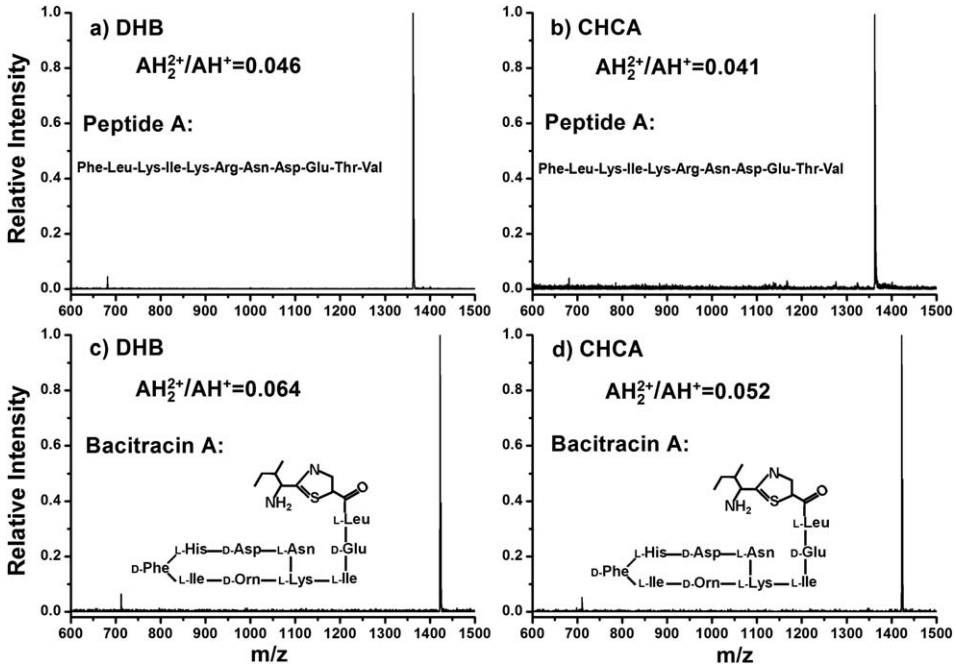

Fig. 1 Spectra and relative intensities of doubly and singly charged ions of peptide A in matrices of (a) DHB and (b) CHCA, and bacitracin A in matrices of (c) DHB and (d) CHCA. The laser irradiance was 7.6×10^7 W cm^{-2}; each spectrum is the accumulation of 600 laser shots.

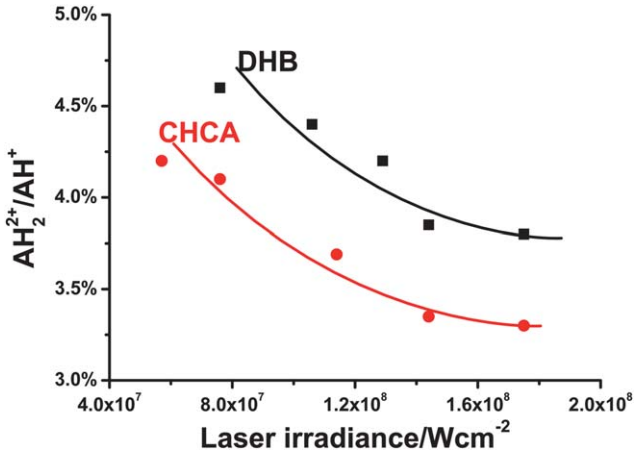

Fig. 2 Influence of laser irradiance on the AH_2^{2+}/AH^+ ratio of peptide A in matrices of DHB and CHCA. Each data point is from the accumulation of 600 laser shots.

should result from the species AH_2^+, as shown in Fig. 3. All the spectra are accumulated from 600 laser shots. We have tried 100, 200, 300, and 600 shots for the isotopic ratio variations, which are 4.5, 1.9, 1.2, and 0.9%, respectively. This is unique evidence supporting the three-body recombination mechanism. If AH_2^+ ions were generated from the two-body recombination as:

$$AH_2^{2+} + e^- \rightarrow AH_2^+ \quad (12)$$

This AH_2^+ production route, also known as electron capture process, is only possible when the molecule is large enough to possess large degrees of freedom. Small peptides, such as peptide A in the experiment, have insufficient degrees of freedom and will not be stable after the absorption of excess energy. More often, fragmentation will be induced.[5] From Fig. 1, only the matrix ion species and the analyte ions are presented in the spectrum with no massive dissociation products observed. Therefore, for small molecules, two-body recombination can only generate AH^+, which follows eqn (9), and will not produce AH_2^+ in the charge reduction process.

Finally, as the laser irradiance increases, the number density of electrons and matrix molecules also increases, which promotes the three-body recombination. More AH_2^+ will come from the process of eqn (6a) or (b), leading to an increase in the $[A + 2]^+/[A + 1]^+$ intensity ratio. This trend can be observed in the experiment, as shown in Fig. 4

It should be noted that three-body recombination is an important charge-reduction process for small molecules in the MALDI plume. Charge-reduction processes can be very complicated when the analyte molecule is large in mass. Multiple recombination mechanisms exist simultaneously. The two-body recombination, especially the electron capture process, should be the dominant charge reduction mechanism because of the large degrees of freedom in large molecules. The ratio of AH_2^{2+}/AH^+ will be much higher than that predicted from three-body recombination because of the large amount of protonation sites and large degrees of freedom in large molecules, such as the lysozyme spectrum shown in Fig. 5. Even triply charged ions are commonly observed. In a word, the influence of the three-body recombination mechanism decreases with the increase of the mass of analyte molecules.

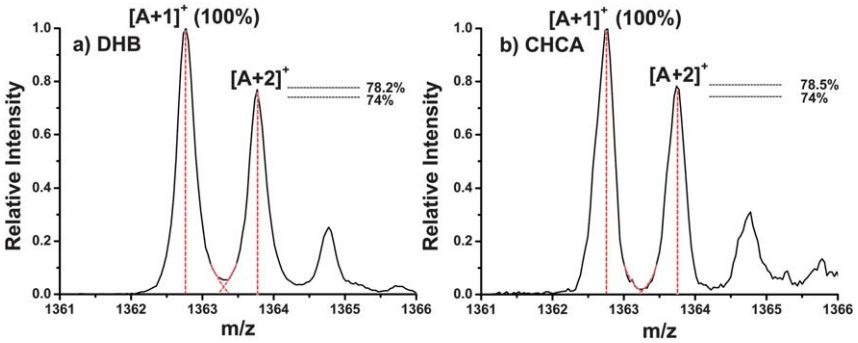

Fig. 3 The isotopic distribution of peptide A in matrices of (a) DHB and (b) CHCA. The laser irradiance was 7.6×10^7 W cm^{-2}; each spectrum is the accumulation of 600 laser shots.

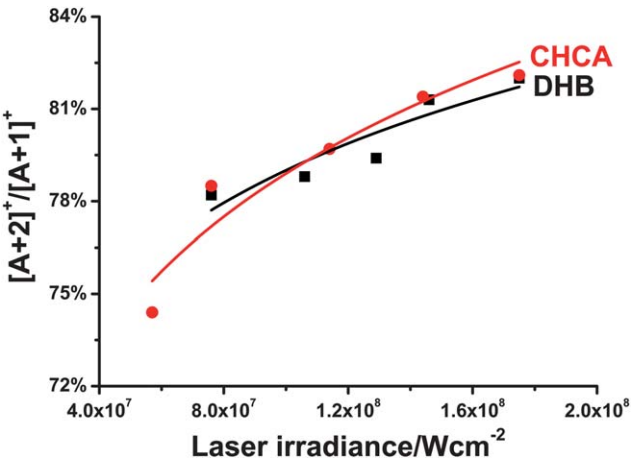

Fig. 4 Dependence of $[A + 2]^+/[A + 1]^+$ intensity ratio on the laser irradiance for peptide A in matrices of DHB and CHCA. Each data point is from the accumulation of 600 laser shots.

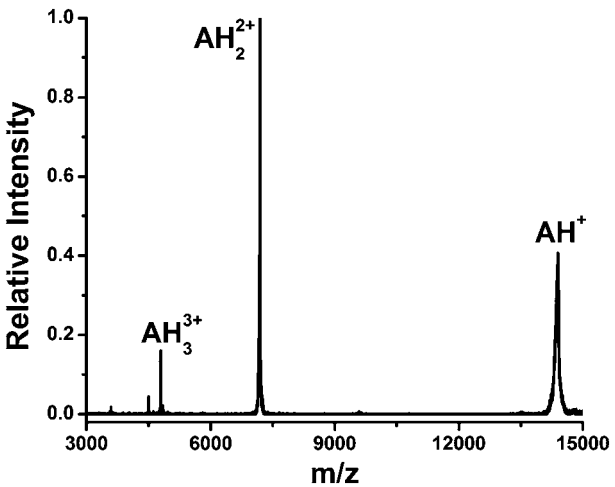

Fig. 5 Mass spectrum of lysozyme in matrix CHCA at laser irradiance of 1.1×10^8 W cm^{-2}. The spectrum is from the accumulation of 600 laser shots.

Conclusions

In summary, three-body recombination is suggested to be an important charge reduction mechanism for small molecules in the MALDI events. Electrons originating from either multiphoton ionization or the energy pooling processes play a significant role in the recombination process. Both the high number density and the low temperature of electrons in the plume ensure the high recombination rate for three-body recombination collisions. Ions with a higher charge state will be much more easily recombined, leaving singly charged ions as the dominant ion species. It must be emphasized that three-body recombination mechanism could play a significant role in charge reduction only for small analyte molecules with insufficient degrees of freedom. For large molecules, the excess energy of the two-body recombination is easily taken up in the large degrees of freedom. Therefore, the two-body recombination undoubtedly dominates over the three-body recombination in the charge reduction of large molecules.

Acknowledgements

Financial support was provided by Natural Science Foundation of China Financial (no. 20775063 and 21027011) and NFFTBS (no. J1030415).

References

1 M. Karas, D. Bachmann, U. Bahr and F. Hillenkamp, *Int. J. Mass Spectrom. Ion Processes*, 1987, **78**, 53–68.
2 R. Knochenmuss, *J. Mass Spectrom.*, 2002, **37**, 867–877.
3 R. Knochenmuss, *Anal. Chem.*, 2003, **75**, 2199–2207.
4 M. Karas and R. Krüger, *Chem. Rev.*, 2003, **103**, 427–440.
5 M. Karas, M. Glückmann and J. Schäfer, *J. Mass Spectrom.*, 2000, **35**, 1–12.
6 H. Ehring, M. Karas and F. Hillenkamp, *Org. Mass Spectrom.*, 1992, **27**, 472–480.
7 P. C. Liao and J. Allison, *J. Mass Spectrom.*, 1995, **30**, 408–423.
8 Y. Huang and D. H. Russell, *Int. J. Mass Spectrom. Ion Processes*, 1998, **175**, 187–204.
9 K. Dreisewerd, M. Schürenberg, M. Karas and F. Hillenkamp, *Int. J. Mass Spectrom. Ion Processes*, 1995, **141**, 127–148.
10 R. Knochenmuss and R. Zenobi, *Chem. Rev.*, 2002, **103**, 441–452.
11 L. V. Zhigilei and B. J. Garrison, *Appl. Phys. Lett.*, 1999, **74**, 1341–1343.
12 R. Knochenmuss, A. Stortelder, K. Breuker and R. Zenobi, *J. Mass Spectrom.*, 2000, **35**, 1237–1245.
13 V. Karbach and R. Knochenmuss, *Rapid Commun. Mass Spectrom.*, 1998, **12**, 968–974.
14 R. Knochenmuss, *Analyst*, 2006, **131**, 966–986.

15 R. Knochenmuss and L. V. Zhigilei, *J. Phys. Chem. B*, 2005, **109**, 22947–22957.
16 R. Zenobi and R. Knochenmuss, *Mass Spectrom. Rev.*, 1998, **17**, 337–366.
17 T. J. D. Jorgensen, G. Bojesen and H. Rahbek-Nielsen, *Eur. J. Mass Spectrom.*, 1998, **4**, 39–45.
18 D. S. Gross and E. R. Williams, *J. Am. Chem. Soc.*, 1995, **117**, 883–890.
19 V. Frankevich, J. Zhang, M. Dashtiev and R. Zenobi, *Rapid Commun. Mass Spectrom.*, 2003, **17**, 2343–2348.
20 R. Knochenmuss, *Anal. Chem.*, 2004, **76**, 3179–3184.
21 N. D'Angelo, *Phys. Rev.*, 1961, **121**, 505–507.
22 R. Huang, Q. Yu, L. Li, Y. Lin, W. Hang, J. He and B. Huang, *Mass Spectrom. Rev.*, 2011, **30**, 1256–1268.
23 L. M. Biberman, V. S. Vorob'ev and I. T. Yakubov, *Sov. Phys. Usp.*, 1973, **15**, 375–394.
24 A. Bogaerts, R. Gijbels and R. J. Carman, *Spectrochim. Acta, Part B*, 1998, **53**, 1679–1703.
25 D. A. Allwood, P. E. Dyer, R. W. Dreyfus and I. K. Perera, *Appl. Surf. Sci.*, 1997, **109–110**, 616–620.
26 A. Bellomio, M. a. R. Rintoul and R. D. Morero, *Biochem. Biophys. Res. Commun.*, 2003, **303**, 458–462.